Journal of Translational Medicine

RESEARCH

Open Access

Identification of the metabolic protein ATP5MF as a potential therapeutic target of TNBC

Kaiyan Chen[1,2†], Yingchun Wu[3†], Linfeng Xu[1†], Changyong Wang[4*] and Jinqiu Xue[1*]

Abstract

Background Triple-negative breast cancer (TNBC), a distinct subtype of breast cancer, is characterized by its high invasiveness, high metastatic potential, proneness to relapse, and poor prognosis. Effective treatment regimens for non-*BRCA1/2* mutation TNBC are still lacking. As a result, there is a pressing clinical necessity to develop novel treatment approaches for non-BRCA1/2 mutation TNBC.

Methods For this research, the scRNA data was obtained from the GEO database, while the transcriptome data was obtained from the TCGA and *METABRIC* databases. Quality control procedures were conducted on single-cell sequencing data. and then annotation and the Copycat algorithm were applied for anlysis. Employing the high dimensional weighted gene coexpression network analysis (hdWGCNA) method, we analyzed the tumor epithelial cells from non-*BRCA1/2* mutation TNBC to identify the functional module genes. PPI analysis and survival analysis were further emplyed to identify the key gene. siRNA-NC and siRNA-ATP5MF were transfected into two MDA-MB-231 and BT-549 TNBC cell lines. Cell growth was determined by CCK8 assay, colony formation and migration assay. Electron microscopy was used to examine the structure of mitochondria in cells. JC-1 staining was used to measure the potential of the mitochondrial membrane. A tumor xenograft animal model was established by injecting TNBC cells into nude mice. The animal model was usded to evaluated in vivo tumor response aftering ATP5MF silencing.

Results Using hdWGCNA, we have identified 136 genes in module 3. After PPI and survival analysis, we have identified ATP5MF as a potential therapeutic gene. High ATP5MF expression was associated with poor prognosis of non-*BRCA1/2* mutation TNBC. The high expression of ATP5MF in TNBC tissues was evaluated using the TCGA database and IHC staining of clinical TNBC specimens. Silencing ATP5MF in two TNBC cell lines reduced the growth and colony formation of TNBC cells in vitro, and hindered the growth of TNBC xenografts in vivo. Additionally, ATP5MF knockdown impaired mitochondrial functions in TNBC cells.

Conclusion In summary, the metabolic protein ATP5MF plays a crucial role in the non-BRCA1/2 mutation TNBC cells, making it a potential novel diagnostic and therapeutic oncotarget for non-BRCA1/2 mutation TNBC.

†Kaiyan Chen, Yingchun Wu and Linfeng Xu contributed equally to this work.

*Correspondence:
Changyong Wang
13814069669@163.com
Jinqiu Xue
xuejinqiu_1986@163.com
Full list of author information is available at the end of the article

Introduction

Breast cancer (BC) ranks the most frequently diagnosed cancer in women and the second most common cause of cancer-related deaths globally. BC is classified into three main subtypes based on molecular markers, such as estrogen receptor (ER), progesterone receptor (PR), and human epidermal growth factor receptor 2 (HER2). The three major subtypes of BC include HR-positive, HER2-positive and triple-negative breast cancer (TNBC). TNBC makes up around 15–20% of all cases of BC [1]. Unfortunately, individuals diagnosed with the TNBC subtypes tend to have a more aggressive nature, resulting in a decreased overall prognosis compared to other subtypes [2].

TNBC, in contrast to other types of BC, has few treatment choices and is susceptible to recurrence and metastasis. TNBC patients also tend to have poor prognosis [3, 4]. The primary cause is the absence of ER, PR and HER2 expression, rendering endocrine therapies and targeted treatments ineffective. As a result. chemotherapy is now the primary method used to treat TNBC [5]. A lack of homologeous recombination, linked to the loss of the breast cancer susceptibility gene(BRCA) in breast cancer, has been confirmed to be related to a positive reaction to cisplatin therapy. Individuals harboring germline *BRCA1/BRCA2* mutations exhibited a heightened response rate (RR) of 54.5% (95% confidence intercal, CI, 23.4 to 83.3%), indicating that a subset of TNBC patients with BRCA1/2 mutation derive significant advantages from platinum-based treatments, underscoring the importance of assessing tumor DNA repair capabilities [1]. Recent findings indicate that TNBC is characterized by augmented cell growth, increased immune cell infiltration, basal-like and mesenchymal traits and impaired homologous recombination due to *BRCA1* dysfunction [6]. TNBC is commonly associated with pathogenic mutations of *BRCA1* and *BRCA2*. Only approximately 7–20% of individuals diagnosed with TNBC carry hereditary mutations in the *BRCA1* or *BRCA2* genes [7]. Therefore, it is crucial to discover novel drug targets for non-*BRCA1/BRCA2* mution TNBC.

High dimensional weighted gene coexpression network analysis (hdWGCNA) was developed to conduct weighted gene co-expression network analysis (WGCNA) on single-cell data [8]. The hdWGCNA method helped in finding robust modules of interconnected genes in single-cell sequencing data [9]. hdWGCNA blends the hierarchical cluster analysis(HCA) and WGCNA. Considering the majority of human breast cancers arise from the transformation of epithelial cells [10], hdWGCNA allowed for discovering modules of TNBC epithelial cells that are difficult to identify by traditional clustering methods and provided a new way to deeply understand epithelial cell heterogeneity and function.

In the study, our goal is to use hdWGCNA to discover important modules and genes that are essential in non-*BRCA1/BRCA2* mutation TNBC, which helps to uncover potential new treatment targets for non-*BRCA1/BRCA2* mutation TNBC.

Materials and methods

Datasets acqusition

The scRNA-seq data we used in the study were sourced from the Gene Expression Omnibus (GEO) database, specifically from GSE161529. GSE161529 contained 11 normal samples, 4 triple negative tumor samples with *BRCA1/2* mutation, 4 triple negative tumor samples without *BRCA1/2* mutation, 11 luminal tumor samples and 10 HER2 positvie tumor samples. To analyze ATP5MF mRNA expression in breast cancer patients, we obtained ATP5MF transcriptome level of samples from TCGA dataset, including 114 normal tissues, 566 luminal tumor tissues, 37 HER2 positvie tumor tissues and 116 triple negative tumor tissues. Clinical data and sequencing data of 235 TNBC patients from *METABRIC* database was used for further survival analysis. Transcriptome data of 235 non-BRCA mutation TNBC and 1,745 other types of breast cancer from *METABRIC* dataset was used for differential analysis.

CMAP analysis

CMAP (http://www.broadinstitute.org/cmap/) is a database containing information on small molecule medications, gene expression and biological uses related to various diseases [11]. By utilizing CMAP analysis, gene expression profiles were compared in order to discover drugs closely associated with diseases, determine the primary chemical compositions of the majority of drug molecules and outline potential mechanisms of these drug molecules. The study analyzed highly expressed DEGs in non-*BRCA1/BRCA2* mutation TNBC, using CMAP to identify potential small molecule drugs for treatment. A threshold of |connectivity score| >0.7 was established to pinpoint potential small molecule drugs linked to non-BRCA mutation TNBC as described in previous articles [12, 13] .

Molecular docking verification and domain prediction

Molecular docking is a commonly used technique to study how small molecules interact with target proteins and evaluate their affinities at particular binding locations. Download molecular structure files of Oligomycin A, Oligomycin C, piceatannol using the Pubchem database. The PDB database was used to find and download the molecular structure file of the target

protein ATP5MF. Download molecular structure files for ATP5MF using the Pubchem database. The downloaded target proteins underwent processing with PyMOL2.3.0 software in order to eliminate water molecules and original ligands. Molecular mechanics optimization of the optimal conformation of all molecules was performed using Chem3D (2020 edition) software, and finally we obtained the optimal conformation with minimal energy.

scRNA-Seq quality control and integration

Analysis of the scRNA-seq data was performed with Seurat (v4.3.0). Quality control measures were applied by excluding cells with mitochondrial gene expression levels exceeding 15% and detected gene counts falling below 300 or exceeding 5000. Subsequently, the remaining cells underwent additional analytical procedures including normalization, identification of highly variable genes, scaling, and principal component analysis (PCA). We used the harmony package following its official instructions to remove the batch effect from our merged scRNA-seq data. After completing the process of harmonious integration, we utilized the RunUMAP function to conduct uniform manifold approximation and projection (UMAP). Cell clusters were identified using the FindNeighbors and FindClusters (resolution = 0.2) functions. Default parameters were used for all standard analysis procedures.

Cell annotation

In order to guarantee the precision of cell labeling, we employed the FindAllMarkers function to detect differentially expressed genes (DEGs) within each cluster. Predefined markers from existing literature were utilized to form a thorough assessment of the final cell type (see Supplementary Figure S1). Specifically, epithelial cells are represented by EPCAM, T cells by CD3, B cells by CD19, plasmablasts by JCHAIN, myeloid by CD68, endothelial cells by VWF and PECAM1 and fibroblasts by PDGFRA and PDGFRB.

High-dimensional weighted correlation network analysis

To further identify tumor cells and somatic cells from epithelial cells, copy number variations (CNV) were detected using copyKat version 1.6.10. The CopyKAT(Copy number Karyotyping of Aneuploid Tumors) algorithm assists in distinguishing between the aneuploid tumor cells and diploid normal cells. Subsequently, 13,616 epithelial tumor cells from triple-negtive breast cancer without *BRCA1/2* mutation were used for hdWGCNA. The hdWGCNA package (version 0.2.2) developed by Morabito et al. was utilized for conducting weighted gene co-expression network analysis (WGCNA) on single-cell data [14]. Initially, genes expressed in a minimum of 5% of cells were inputted, followed by the application of the 'MetacellsByGroups' function to generate the metacell gene expression matrix. Subsequently, the optimal soft power was determined using the 'TestSoftPowers' function, and the co-expression network was constructed using the 'ConstructNetwork' function. The analyses were carried out according to the official standard procedure outlined at https://smorabit.github.io/hdWGCNA/articles/basic_tutorial.html.

Protein-protein interactions (PPI) and functional enrichment analysis

A total of 136 genes in module 3 underwent protein-protein interaction analysis in the STRING database and the Cytoscape 3.9.1 software was utilized for visualization. Functional enrichment analysis was performed using the R "clusterProfiler" package. After PPI analysis of the module 3 genes, the K-means clustering algorithm was performed and we obtained three main clusters. Cluster 1 is the main cluster associated with ATP metabolic process, and the top 10 key genes of cluster 1 were obtained by further PPI analysis.

Survival analysis

Survival analysis of non-BRCA1/BRCA2 TNBC patients based on ATP5MF expression level was performed utilizing the "survival" and"survminer" packages. We set the significance level at a P value of 0.05. Kaplan-Meier(KM) analysis was performed to plot survival curves using the R software. The conf.type parameter was set to 'log', applying the log-rank test to compare survival differences between the two groups. All the data was from *METABRIC* dataset and TCGA dataset.

Animal xenograft studies

Female nude mice' flanks were injected with six million TNBC cells per mouse were subcutaneously (s.c.). After 7 days, the subcutaneous xenografts had developed to approximately 100 mm^3 each (referred to as 'Day-0'). Oligomycin (HY-N6782, MCE) was given at a dose of 40 ml/kg subcutaneously twice a day for 2 weeks. Xenograft volumes, animal body weights, and daily tumor growth (in mm^3 per day) were estimated. Nude mice were acquired from the Model Animal Research Center of Nanjing University (Nanjing, China) with approval from the Institutional Animal Care and Use Committee of Nanjing Medical University.

Clinical specimens and tissue samples

Fresh samples of breast cancer tissues were collected during the specified time frame. In the hospital, healthy tissue samples near cancer ($n = 10$), luminal tumor samples ($n = 6$), HER + tumor samples ($n = 5$), and TNBC

tumor samples ($n=9$) were collected. Prior consent from patients and approval from the Ethics Committee of the Second Affiliated Hospital of Nanjing Medical University were obtained for the use of these clinical materials. Two pathologists made all the diagnoses following the guidelines of Pathology and Genetics of Tumors of the Breast and Female Genital Organs of the World Health Organization Classification of Tumors.

Immunohistochemical staining

The sections from tissue samples of clinical specimens were used for detection of the expression of ATP5MF. Following dewaxing and performing antigen retrieval, the sections were incubated with an ATP5MF antibody (68128-1-Ig, Proteintech, China).

After being stored at 4 ℃ overnight, the samples were then treated with secondary antibody (A0277, Beyotime, China) for 1 h at 37 ℃. View and capture images under a microscope. We used the IRS (Immunoreactive Score) scoring method to score immunohistochemical staining. Scoring was performed by determining the intensity of staining and the percentage of positive cells, and a final score of ≥ 3 was classified as a high expression group and < 3 as a low expression group.

Cell viability assay

We assessed cell viability using the CCK8 assay according to the manufacturer's instructions. Cells were seeded at a density of 10^4 cells per well in 24-well plates containing 500 μl of DMEM. Following the specified treatment, CCK8 reagents from Beyotime Biotechnology were introduced to the culture medium and incubated for 2–3 h. Subsequently, the optical densities of the wells were measured at 450 nm using a microplate reader. The percentage of cell viability was determined by comparing the experimental cells to normal cells.

Cell culture

Several classical triple-negative breast cancer cell lines (MDA-MB-231, BT-549, MDA-MB-468, BT-20, Hs 578T, HCC1806) were acquired from the Chinese Academy of Sciences (Shanghai, China). Cells were cultured with Dulbecco's Modified Eagle Medium (DMEM) supplemented with 10% fetal bovine serum (FBS) and 1% penicillin at 37 °C and in a 5% CO_2 atmosphere.

siRNA transfection

GenePharma (Shanghai, China) provided oligonucleotides that encode siRNA targeting ATP5MF (siATP5MF 5-CUACCGGUACUACAACAAGTT-3) as well as control siRNA. siRNA-NC (si-NC 5-UUCUCCGAACGU GUCACGUTT-3) was transfected simultaneously as a control to ensure siRNA-ATP5MF specificity. The transfection of siRNA was performed using the Lipo2000 transfection reagent (11668-019, Invitrogen, USA) according to the supplier's protocol.

Colony formation assay

Following a 48-hour transfection, we seeded cells in 6-well plates at a low density (around 500 cells per well) and permitted cells to proliferate for 14 days. The medium was replaced every three days to ensure nutrient availability and optimal growth conditions. Following the period of incubation, colonies were treated with 4% paraformaldehyde for 15 min and then stained using 0.1% crystal violet for 20 min. Any extra stain was removed by rinsing with water, and the plates were then allowed to air dry. The stained colonies were manually counted using a colony counter. Only colonies with more than 50 cells were included in the count to ensure that the colonies arose from single cells and represented true clonal expansion. The results were expressed as the number of colonies formed per well.

Transwell Assay

The migration and invasion abilities of breast cancer cells were assessed using 24-well transwell inserts (Millicell Hanging Cell Culture Insert, USA). A 200 μl cell suspension in serum-free DMEM was added to the upper chamber, while 600 μl medium containing 10% FBS served as the chemoattractant in the lower chamber. After incubation at 37 ℃ for 24–48 h, the cells that successfully invaded or migrated were stained with 1% crystal violet for analysis.

ATP Measurement Assay

We incubated cells for additional 24 h to allow for cellular processes to stabilize. Following the completion of treatments, the cells were rinsed with cold phosphate-buffered saline (PBS). Subsequently, the ATP assay Kit (S0026, Beyotime, China) was employed to quantify ATP levels in the cell lysates through a colorimetric assay in accordance with the manufacturer's guidelines. The obtained results were subsequently normalized based on the protein concentrations of the individual tests.

Quantitative real-time PCR (qRT-PCR)

TRIzol (Takara, Dalian, China) reagents were utilized for RNA extraction. RNA was utilized for reverse transcription reactions and quantitative real-time PCR following the guidelines provided by the manufacturer. The experiments were repeated in triplicate, at minimum.

Western blotting

Cells were lysed using radio immunoprecipitation assay and PMSF (Biocolors, Shanghai, China) and quantified

with the BCA protein assay kit (Merck, Darmstadt, Germany). Equivalent quantities of protein were then separated on an SDS gel and transferred to PVDF membranes (Millipore, Bedford, MA, USA). Signal detection was performed using a Luminescent Image analyzer (GE Healthcare Bio-Sciences, Uppsala, Sweden), with β-Actin serving as the control.

Transmission electron microscopy (TEM)

We initially plated cells in 6-well plates at a concentration of 5×10^5 cells per well and subsequently immobilized the cells for transmission electron microscopy (TEM) analysis. The immobilized cells were further treated with a 1% OsO4 buffer, dehydrated in a series of alcohol solutions, and embedded in epon resin. Subsequently, we prepared ultrathin Sect. (100 nm) of the cell samples and stained cells with 3% lead citrate plus uranyl acetate, and examined cells using an electron microscope (JEOL JEM-1400Flash).

Detection of mitochondrial membrane potential

The changes in mitochondrial membrane potential were determined using JC1 fluorescent dye by a flow cytometry. Following a 24-hour transfection period, the cells were treated with JC-1 dye at a concentration of 2.5 μg/mL and incubated at 37 ℃ in the absence of light for 20 min. Following the staining process, the cells were rinsed with PBS in order to eliminate any surplus dye. The flow cytometer was set up to detect JC-1 monomers and aggregates. The intensity of green fluorescence (JC-1 monomers) was detected at 485/535 nm, while the intensity of red fluorescence(JC-1 aggregates) was detected at 540/570 nm. The JC-1 aggregates/monomers ratio was used to express the results. A reduction in the ratio of fluorescence intensity between polymer and monomer indicated mitochondrial depolarization.

Statistical analyses

Statistical analyses were conducted with SPSS version 23.0 (SPSS, USA) and GraphPad Prism 8.0 (GraphPad Software, USA). Significance of variations was assessed using independent t-tests or one-way ANOVA with Tukey's post-test. A p-value below 0.05 (two-tailed) was deemed to be statistically significant, suggesting the existence of significant results. We analyzed the categorical data statistically using the fisher exact probability method. SPSS was used for statistical analysis and $p<0.05$ was considered statistically significant.

Results

scRNA-seq analysis unveiled the composition of tumor cells across various subtypes of breast cancer

We initiated the processing and analysis of the sequencing data for TNBC. After conducting quality control, we selected the first 14 principal components for further exploration through PCA. Utilizing UMAP dimensionality reduction, we identify 8 distinct cell subsets (Fig. 1A). Due to most breast cancers are of epithelial cells, we obtained a Seurat matrix comprising 112,037 epithelial cells, including 49,765 normal epithelial cells, 19,968 ER positive breast cancer epithelial cells, 16,352 luminal breast cancer epithelial cells and 25,952 TNBC epithelial cells. In order to filter out normal epithelial cells, Copycat algorithm was further used to identify aneuploid epithelial cells and diploid epithelial cells (Fig. 1B). We defined aneuploid cells as tumor cells and diploid epithelial cells as normal cells. The left plot of Fig. 1C depicted the original distribution and clustering of the epithelial cells within the samples. The right plot of Fig. 1C focused on the TNBC tumor cells after Copycat algorithm. As a result, a total of 13,616 breast cancer epithelial cells from TNBC tumor tissues without *BRCA1/2* mutations were identified for further hdWGCNA analysis.

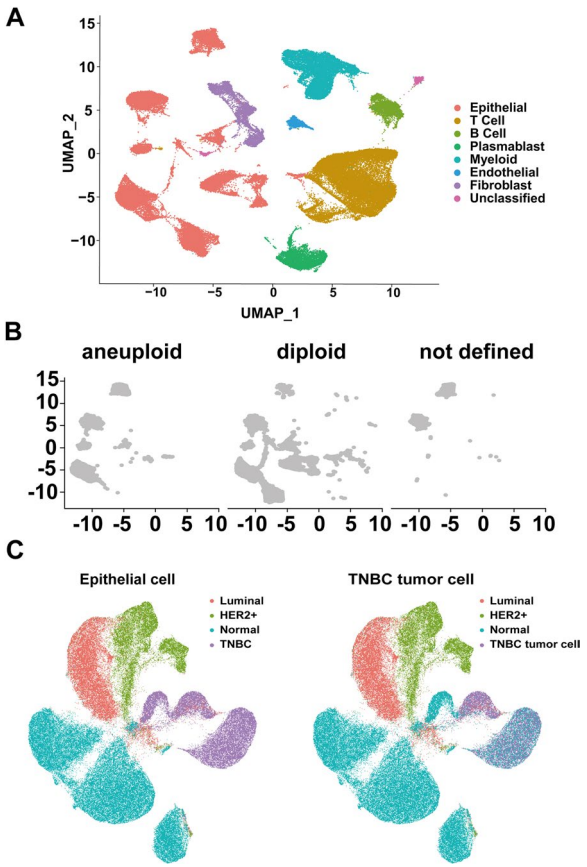

Fig. 1 Normal breast tissue and breast tumors in scRNA-seq characterization. **A** The distribution of various kinds of cells in breast tissues from breast cancer patients and normal samples. **B** CopyKat algorith result of all kinds of epithelial cells. **C** Clustering of the epithelial cells before and after using CopyKat

Identification of ATP5MF as the key gene in TNBC without *BRCA1/2* mutation based on hdWGCNA

Subsequently, we constructed a co-expression network using scRNA-seq data with the best soft threshold set at 5, as illustrated in Fig. 2A. The connectivity between modules was assessed by examining the unique genes present in each module. As a result, we identified 11 non-gray modules (Fig. 2B). It is well established that we often focus on "hub genes" in hdWGCNA analysis, which is highly connected within each module. Therefore, our goal was to calculate the kME, which represents the eigengene-based connectivity of genes. We visualized the top ten genes in each module ranked by kME (Fig. 2C). The enrichment fraction of these distinctive genes in each cell subgroup was visualized in

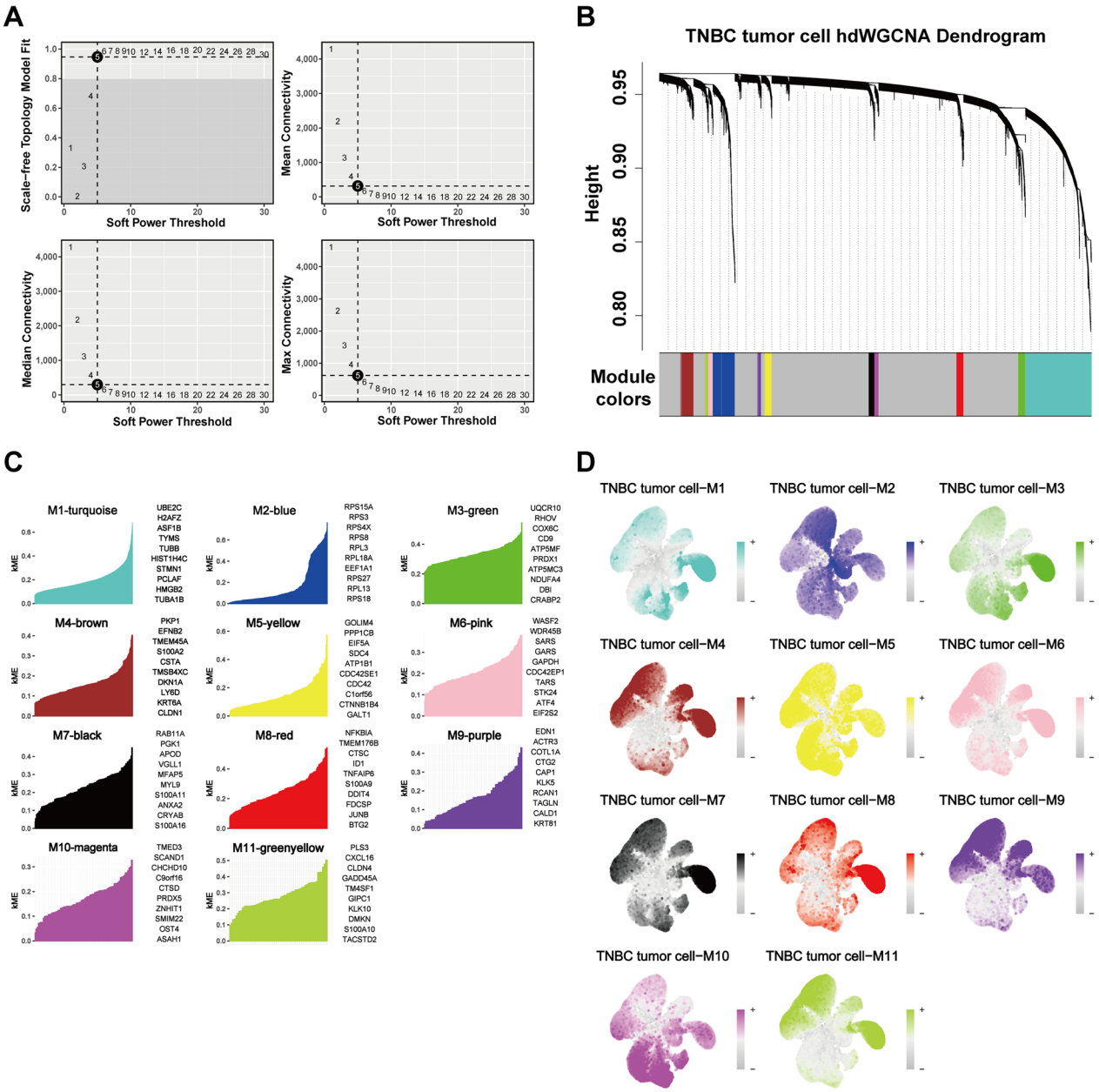

Fig. 2 hdWGCNA analysis of the epithelial cell genes in non-***BRCA1/BRCA2***mutation TNBC. **A** The selection of the best soft threshold. **B** Construct a co-expression network using the optimal soft threshold of 5 and divide the genes into distinct modules in order to generate a gene clustering tree. **C** Calculate the feature-based gene connectivity of each gene in the co-expression network analysis to determine the highly connected genes in each module. **D** Gene scores for each module gene are determined using the UCell algorithm

Fig. 2D. The result indicated that Module 3 was specifically elevated in TNBC tumor epithelial cells.

The correlation between modules was depicted in Fig. 3A. Notably, among all 11 modules, module 3 showed strong associations with other modules, indicating its important role. The result of bubble plot of 11 modules expression in 4 clusters of epithelial cells indicated that module 3 was especially high expressed in epithelial cells form TNBC without *BRCA1/2* mutation (Fig. 3B). The results showed that genes in Module 3 played a key role in TNBC without *BRCA1/BRCA2* mutations.

GO and KEGG analysis of the 136 genes in module 3 were performed. The GO functional and KEGG pathway enrichment analysis revealed that 131 GO-BP terms, 81 GO-CC terms, 50 GO-MF terms, and 16 KEGG terms were enriched by the genes in module 3, and the top 3 terms of each category are represented in Figures C. The three BP terms were ATP metabolic process, aerobic respiration and oxidative phosphorylation. The three CC terms were mitochondrial inner membrane, mitochondrial protein-containing complex and inner mitochondrial membrane protein complex. The three MF terms were electron transfer activity, proton transmembrane transporter activity and oxidoreduction-driven active transmembrane transporter activity. Finally, the three KEGG terms were identified as Huntington disease, Parkinson disease and oxidative phosphorylation. Notably, the results of function enrichment analysis indicated the genes in module 3 were mainly related to mitochondrial function and ATP metabolism.

After PPI analysis of the 143 genes of module 3, the K-means clustering algorithm was performed. The main three clusters are obtained with red representing cluster 1, blue representing cluster 2 and green representing cluster 3. The PPI network of these 143 genes was visualized in Fig. 5B. In the PPI network,

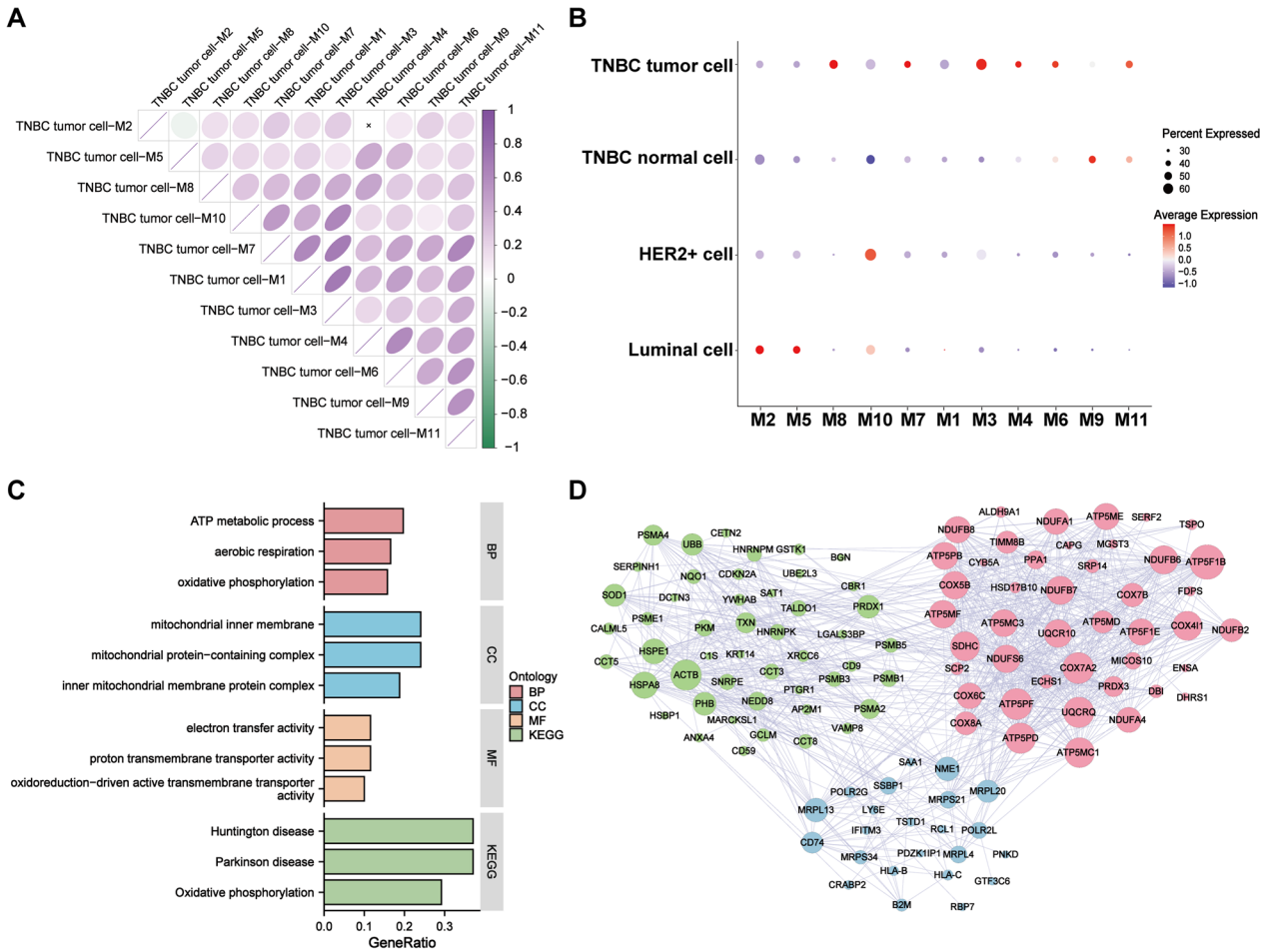

Fig. 3 Identification of the key module of hdWGCNA. **A** Correlation heatmap is shown between different modules. **B** Bubble plot of 11 modules expression in 4 clusters of epithelial cells. The size of each bubble corresponds to the percentage of module cells, while the color indicates the average expression level within each cluster. **C** GO and KEGG analysis of genes in module 3. **D** The protein interaction network constructed for the genes in module 3

larger node sizes indicate higher degree values. Obviously, cluster 1 is the most important among the three clusters. Cluster 1 is also the cluster associated with ATP metabolic process, especially ATP synthase and mitochondrial. The top 10 key genes of cluster 1 were obtained by further PPI analysis Fig. 4A.

Using Venn diagram, we take the intersection of the top 10 hub genes in module 3 characterized by high kME and 10 key genes characterized by high degree. As a result, we obtained 2 intersection genes, namely ATP5MF and UQCR10 (Fig. 4B). Clinical data and sequencing data of 235 TNBC without *BRCA1/BRCA2* mutations patients from METABRIC database was used for further survival analysis. The result of univariate Cox regression analyses showed that UQCR10 was not associated with prognosis of TNBC, while ATP5MF was strongly linked to prognosis of TNBC. Therefore, we identified ATP5MF as the key gene in TNBC without *BRCA1/2* mutation.

Highly expressed ATP5MF in TNBC correlates with poor survival and higher histological grade

The Kaplan-Meier survival curve in Fig. 4C indicated that there is a negative correlation between ATP5MF expression level and overall survival, which means the higher the ATP5MF expression level, the worse the outcomes. In order to further complement the survival analysis, we grouped the breast cancer patients in the TCGA database using prognostic covariates related to breast cancer, such as menopausal and status. The results indicated that ATP5MF expression was mostly linked to the prognosis of TNBC patients in different menopause statuses (Supplementary Fig. 2A). The result of the box plot indicated that ATP5MF expression varies significantly across the subtypes (Fig. 4D). Notably, the ATP5MF transcriptome expression is the highest in TNBC, which suggest a potential role of ATP5MF in TNBC. Additionally, the results of IHC staining for ATP5MF verified the highest expression of ATP5MF in TNBC tissues compared with other types of breast cancer (Fig. 4E). Baseline characteristic for 20 breast cancer patients have been included in Table 1.The data was divided into two groups based on

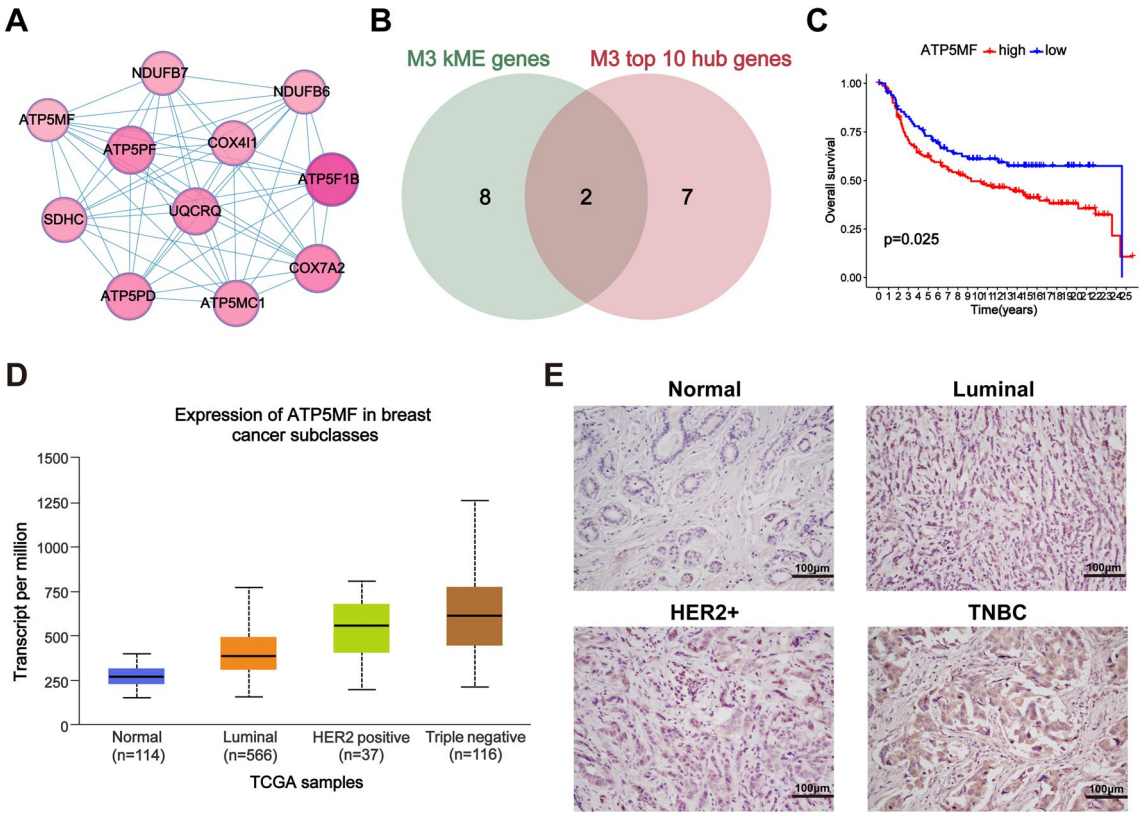

Fig. 4 Identification of ATP5MF as the key gene in non-***BRCA1/BRCA2***mutation TNBC. **A** The PPI network of the ten key genes. **B** Venn diagram of top 10 genes characterized with high kME and top 10 hub genes characterized with high degree. **C** The Kaplan-Meier survival curve of OS and ATP5MF expression. **D** Box plot of the expression of ATP5MF in breast cancer subclasses. **E** IHC results of breast tissue representing each subtype of breast cancer

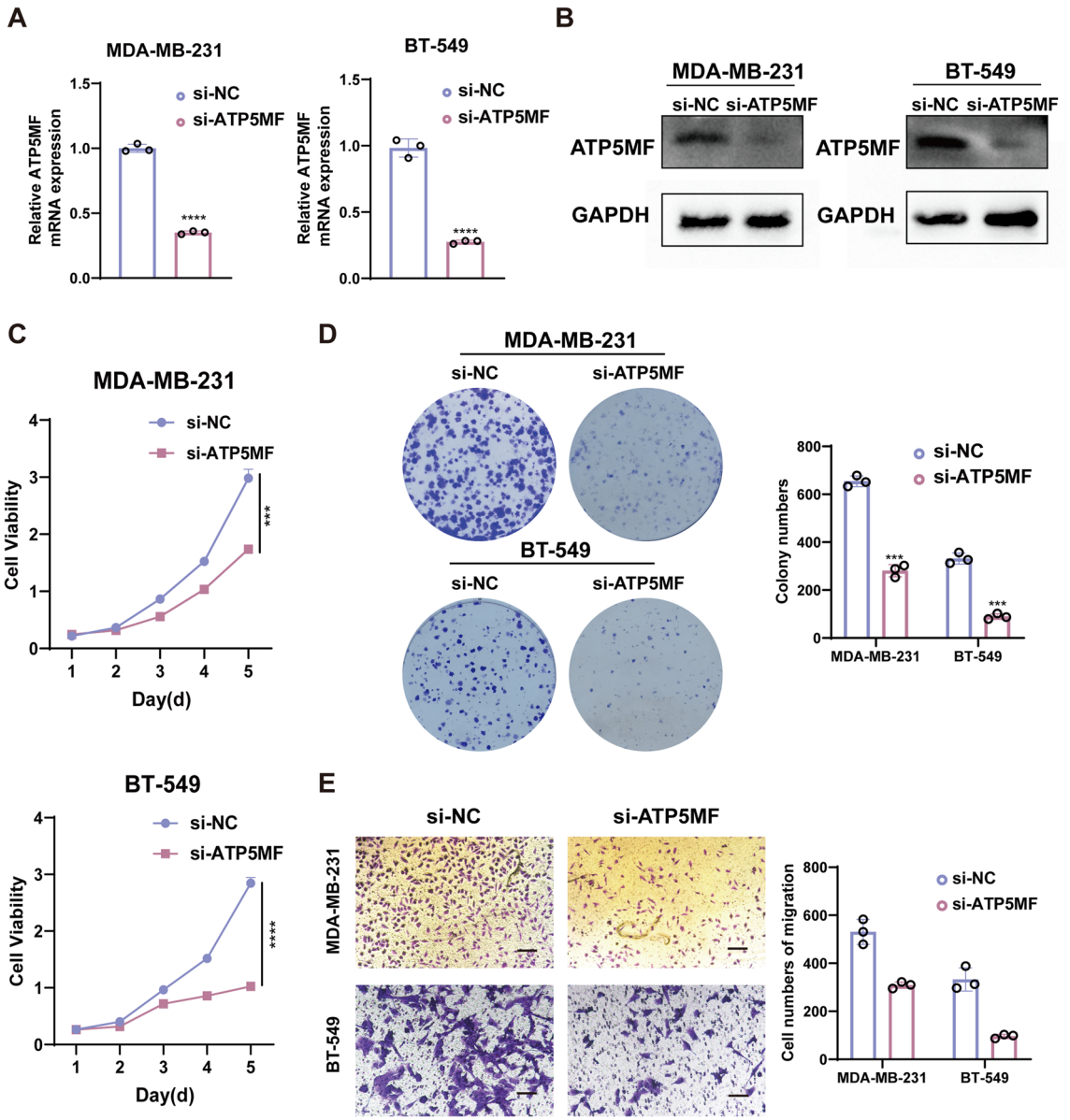

Fig. 5 ATP5MF depletion impedes TNBC cell survival, proliferation and migration. **A** qPCR analysis of ATP5MF. **B** Western blot of ATP5MF. **C** CCK8 assays were tested. **D** Cell cloning assays were tested. **E** Migration ('Transwell' assays) were tested

ATP5MF expression: low and high. The table highlights a significant association with histological grade and ATP5MFexpression. In the group with lower ATP5MF expression, 8 patients had breast cancer with pathological grade II and 2 patients had breast cancer with pathological grade III. In the group with higher ATP5MF expression, 3 patients had breast cancer with pathological grade II and 7 patients had breast cancer with pathological grade III. The higher expression of ATP5MF was linked to higher histological grade($P=0.02$), indicating worse prognosis.

ATP5MF depletion impedes TNBC cell proliferation and migration

MDA-MB-231, BT-549, MDA-MB-468, BT-20, Hs578T and HCC1806 cell lines

were selected to verify the expression of ATP5MF protein. The results showed that MDA-MB-231 and BT-549 had the highest expression (Supplementary Fig. 2B). MDA-MB-231 and BT-549 cells were each transduced with two distinct siRNAs, si-NC and si-ATP5MF, in separate experiments. si-ATP5MF significantly reduced the mRNA and protein levels of ATP5MF in MDA-MB-231

Table 1 Clinical characteristics of patients according to ATP5MF expression in a Breast Cancer Cohort (n = 20).

Characteristic	Low expression of ATP5MF	High expression of ATP5MF	*P* value
n	10	10	
Age			0.99
<=50	3	3	
> 50	7	7	
Tumor size			0.23
< 2	3	2	
2–5	5	8	
> 5	2	0	
Nodal involvement			0.16
0	7	6	
1–3	1	1	
4–9	2	0	
≥ 10	0	3	
Histological grade			**0.02***
I	0	0	
II	8	3	
III	2	7	

and BT-549 cells(Fig. 5A, B). We next tested whether ATP5MF depletion altered breast cancer epithelial cell behaviors. Viability of MDA-MB-231 and BT-549 cells was reduced by ATP5MF silencing as indicated by the CCK-8 assay results (Fig. 5C). The cell clone formation experiment showed a significant decrease in clone formation of MDA-MB-231 and BT-549 cells transfected with si-ATP5MF compared to si-NC. Furthermore, the findings from the 'Transwell' experiment showed a significant decrease in the migration of MDA-MB-231 and BT-549 cells after ATP5MF silencing.

ATP5MF depletion impairs mitochondrial functions in TNBC cells

Previous studies have shown that ATP5MF encodes the f subunit of mitochondrial ATP synthase. Decreasing the human f subunit does not change enzyme stoichiometry or catalysis. However, it is crucial for normal ATP synthase dimer stability, mitochondiral crista morphology and PTP modulation, all of which have significant implications for the cells' ability to handle increased bioenergetic requirements and apoptotic stimuli [15]. Therefore, we investigated the impact of ATP5MF depletion on mitochondrial functions in TNBC cells. Firstly, electron microscopy results showed that swollen mitochondrial with disappeared ridges occured in MDA-MB-231 and BT-549 cells transfected with ATP5MF. These findings suggested that ATP5MF knockdown resulted in mitochondrial impairment (Fig. 6A and B). What's more, JC-1 transitioned from red fluorescence polymers to green fluorescence monomers after ATP5MF silencing. The result indicated that ATP5MF knockdown could lead to mitochondrial depolarization (Fig. 6C). In addition, there i.a. a significant decrease in total ATP level in MDA-MB-231 and BT-549 cells transfected with si-ATP5MF in comparison to the si-NC groups, reflecting a decline in mitochondrial function (Fig. 6D).

Oligomycin, the H+-ATP-synthase inhibitor, inhibits TNBC cell growth in vitro and in vivo

After differential analysis of the 235 non-*BRCA1/BRCA2* mutation TNBC and 1,745 other breast cancer, we identified 81 high expression genes and 49 low expression genes in Module 3 genes. Notably, ATP5MF was included in the 81 high expression genes. GO and KEGG analysis of the 81 high expression was further performed. The results showed that the high expression genes were enriched in ATP metabolism and oxidative phosphorylation (Supplementary Fig. 1). In order to screen out small molecule drugs for treating non-BRCA mutation TNBC by regulating ATP metabolism and mitochondrial function, we imported 81 highly expressed DEGs from Module 3 into the cMAP database. As a result, Oligomycin_A, Oligomycin_C, piceatannol were screened out for further molecular docking analysis. Notably, molecular docking binding energy of Oligomycin_A, Oligomycin_C, piceatannol with ATP5MF was −6.6, −7.5 and −5.7(Fig. 7A). At last, we tested the potential effect of Oligomycin, the H+-ATP-synthase inhibitor in breast cancer.

Western blot results indicated that Oligomycin could inhibit the expression of ATP5MF effectively in a dose-dependent manner (Fig. 7B). Tumor cell viability at different Oligomycin doses was measured by CCK8 assays. The dose-response curves in MDA-MB-231 and BT-549 cells exhibited substantial decreases in cell viability in all groups treated with Oligomycin. Following ATP5MF knockdown, the IC50 values were significantly lower (Fig. 7C). The result indicated that downregulation of ATP5MF increased the sensitivity of tumor cells to Oligomycin.

To investigate the role of ATP5MF in the TNBC growth in vivo, we established subcutaneous xenograft model (Fig. 7D). Then, si-NC or si-ATP5MF was injected to the xenografts. The volumes of si-ATP5MF xenografts were much lower than those of si-NC xenografts (Fig. 7E). As expected, the volumes of xenografts treated with Oligomycin were much lower than those without Oligomycin treatment. Notably, the volumes of xenografts of si-NC group was higher than those of si-ATP5MF group treated with Oligomycin at the same dose(Fig. 7E).

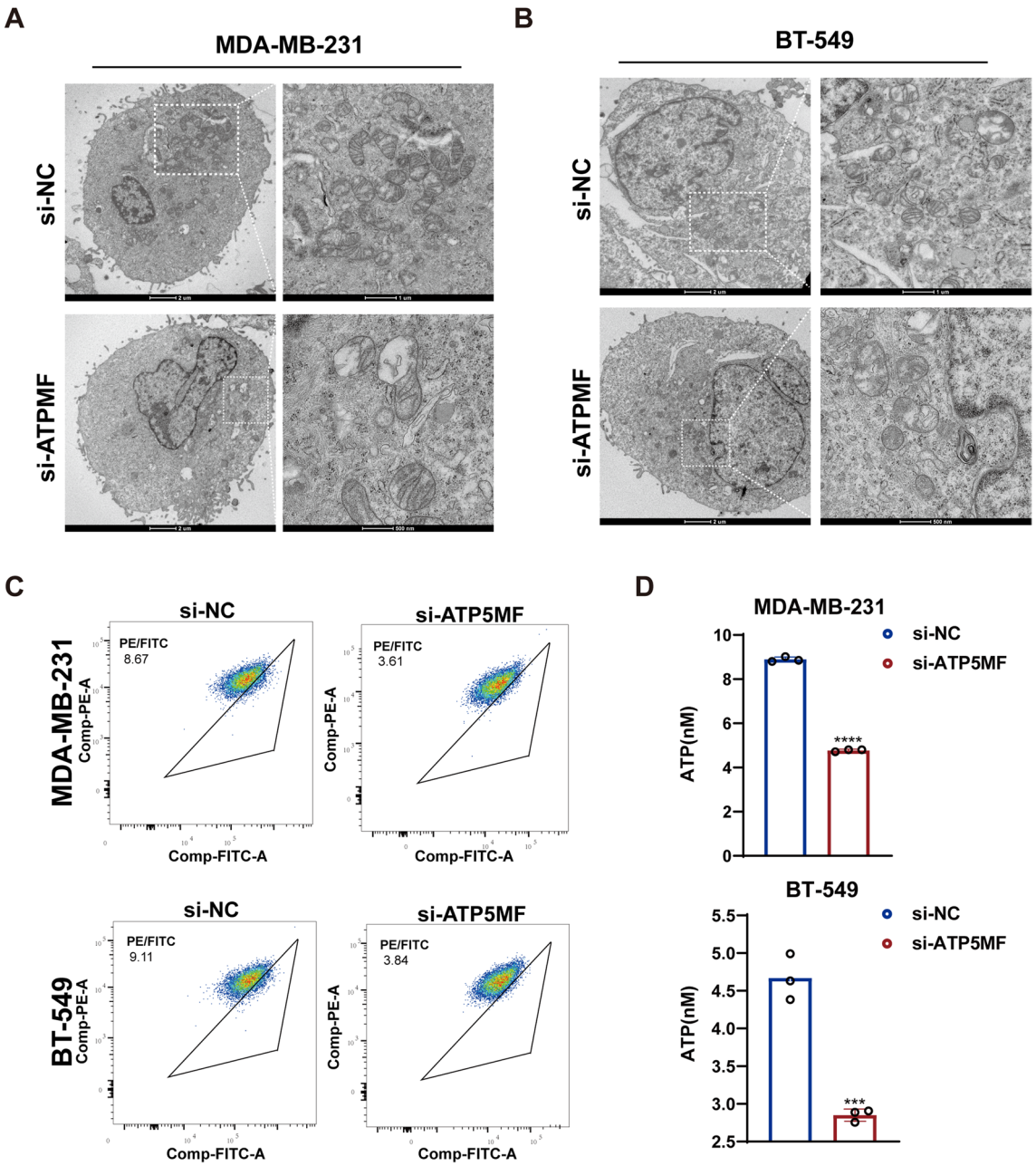

Fig. 6 ATP5MF depletion impairs mitochondrial functions in TNBC cells. **A**-**B** Electron micrographs of mitochondrial in MDA-MB-231 and BT-549 cells. **C** MDA-MB-231 and BT-549 cells were stained with JC-1 and then analyzed using flow cytometry to determine the JC-1 red/green ratio. **D** ATP content was detected

Discussion

It is well established that TNBC patients could not benefit from standard endocrine or HER2-targeted medications because of a lack of necessary receptor markers. The standard of care for non-surgical TNBC remains non-specific chemotherapy. There is an urgent need to meet demands for developing new treatment regime for TNBC [2, 16]. To avoid blind development of therapeutic approaches, numerous studies have been conducted to distinguish the intricate TNBC subtypes and molecular characteristics as these factors are strongly associated with clinical results such as response to chemotherapy, recurrence patterns and prognosis [16]. In 2011, Lehmann et al. conducted gene expression analysis on tumor samples from 587 TNBC individuals and categorized TNBC into six different subtypes: basal-like 1 (BL1),

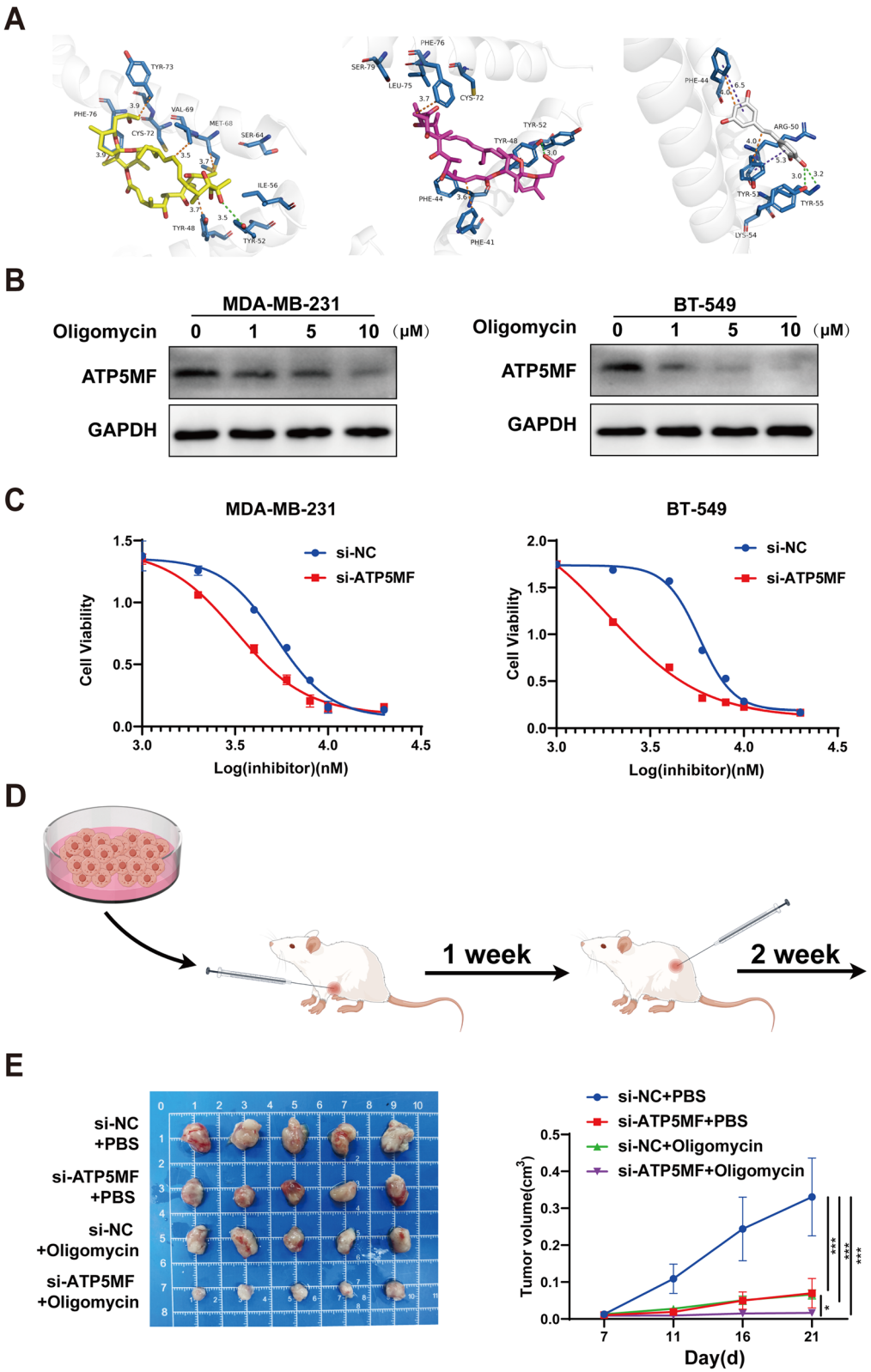

Fig. 7 Oligomycin inhibits TNBC cell growth in vitro and in vivo. **A** Molecular docking of ATP5MF with Oligomycin_A, Oligomycin_C and piceatannol. **B** Western blot of ATP5MF of MDA-MB-231 and BT-549 cells treated with Oligomycin of different concentrations. **C** Cell viability of MDA-MB-231 and BT-549 transfected with si-NC and si-ATP5MF after treatment of Oligomycin. **D** Diagram of animal modeling and treatment. **E** The xenograft volumes were recorded every week

basal-like 2 (BL2), mesenchymal (M), mesenchymal stem-like (MSL), immunomodulatory (IM), and luminal androgen receptor (LAR) [17]. The most recent Fudan classification standard utilized four frequently employed clinical immunohistochemical markers (androgen receptor, CD8, FOXC1 and DCLK1) to categorize TNBC into four transcriptome-based subtypes: luminal androgen receptor (LAR), immunomodulatory (IM), basal-like immune-suppressed (BLIM), and mesenchymal-like (MES) [18]. These categorizations further refine the subtypes of TNBC, opening up new possibilities for targeted treatment and investigating novel therapeutic targets.

This research utilized scRNA-seq analysis and hdWGCNA analysis to gain deeper insights into the biological characteristics and identify potential therapeutic targets for non-*BRCA1/2* mutation TNBC. The hdWGCNA framework was designed for analyzing co-expression network in single-cell and spatial transcriptomics data [19]. Then co-expression networks are created by converting pairwise correlations of input features, which provides a numerical indication of the connection between genes [19, 20]. Analyzing the network structure through hierarchical clustering helps to identify clusters of genes with closely linked expression profiles, which typically correspond to specific biological processes and disease conditions [21, 22]. Due to the fact that different cell types and cell states possess specific gene expression patterns, hdWGCNA was created to support the analysis of cellular and spatial hierarchies at multiple levels. To address these issues, hdWGCNA offers a comprehensive set of tools for analyzing and visualizing data, incorporating biological information from multiple databases to enhance the understanding of co-expression network [23, 24].

In this study, 13,616 breast cancer epithelial cells from TNBC tumor tissues without BRCA1/2 mutations were filtered out after scRNA analysis and Copycat algorithm. After hdWGCNA analysis of non-*BRCA1/2* mutation TNBC epithelial cells, we obtained 11 functional modules. Notably, module 3 was specifically elevated in TNBC tumor epithelial cells. Among all 11 modules, module 3 showed strong associations with other modules, indicating its important role. Moreover, module 3 was especially high expressed in epithelial cells form TNBC without BRCA1/2 mutation. All the results showed that module 3 was the main functional module in non-BRCA1/BRCA2 mutation TNBC. GO and KEGG analysis showed that the module3 genes were mainly enriched in ATP metabolism and mitochondrial morphology. By utilizing a Venn diagram, we identified the top 10 hub genes in module 3 with high kME values and 10 key genes with high degrees. As a result, we obtained 2 intersection genes, namely ATP5MF and UQCR10. In our research, we observed that ATP5MF is overexpressed in non-BRCA1/BRCA2 mutation TNBC. Highly expressed ATP5MF in non-BRCA1/BRCA2 mutation TNBC is linked to poor prognosis and higher histological grade. Therefore, we screened out ATP5MF as the key gene in TNBC without BRCA1/2 mutation.

The ATP5MF gene is responsible for encoding the f subunit of ATP synthase in humans, playing a critical role in both the assembly of ATP synthase and the stability of dimers. Decreasing the human f subunit does not change the ratio of enzymes or their ability to catalyze reactions under typical circumstances. Nevertheless, reducing the f subunit can have harmful effects in situations where there is a need for increased mitochondrial function to fulfill the energy requirements. Proper localization of its key components is crucial for maintaining the stability of the ATP synthase dimer, crista structure and PTP regulation, which has significant implications for the cell's ability to handle increased energy demands and respond to signals that trigger cell death [15]. Research has demonstrated that cancer cells sustain elevated levels of both glycolysis and oxidative phosphorylation (OXPHOS) in order to fulfill the substantial need for energy and substrates required for anabolic processes. The role of mitochondrial energy production is crucial in the initiation and progression of cancer [25, 26].

Various approaches to impede mitochondrial energy production for cancer treatment have been quickly advanced, including disrupting the electron transport chain(ETC), blocking mitochondrial autophagy and causing damage to mitochondrial DNA [27, 28]. Yet, the effectiveness of these promising approaches in fighting cancer is still lacking, largely due to cancer cells relying on both OXPHOS and glycolysis to fulfill their energy needs [29]. Hybrid energy metabolism pathways are present in various areas of the tumor including within individual tumor cells. Furthermore, in the event that a particular route of energy processing is obstructed, an alternative pathway would be triggered to offset the energy deficiency [30]. Prior research emphasized the significance and efficiency of simultaneously blocking OXPHOS and glycolysis, offering new perspectives on cancer treatment.

It has been reported that ATP synthase was an important part of mitochondrial metabolism-related proteins. What's more, ATP synthase was essential both in the process of glycolysis and OXPHOS. Furthermore, it was demonstrated that ATP synthase expression was elevated in TNBC subtype [31]. The findings indicated that ATP synthase plays a crucial function in the metabolic characteristics and biology of TNBC, suggesting it as a promising target for TNBC treatment. In our research, ATP5MF silencing could impedes TNBC cell survival, proliferation and migration. Inhibiting

ATP5MF could lead to energy deficiency, as well as impaired mitochondrial membrane potential and structure. All the results indicated that ATP5MF could be a potential novel therapeutic target for non-*BRCA1/BRCA2* TNBC.

In addition, we screened out Oligomycin as new potential drug by CMAP analysis and molecular docking. Oligomycin could act on the majority of genes in module 3 and could bind to ATP5MF stably and spontaneously. It has been confirmed that Oligomycin as the standard mitochondrial-specific inhibitor could selectively inhibited Glioblastoma Multiforme (GBM) tumors proliferation. Notably, oligomycin has been previously used as an OXPHOS inhibitor together with fucoidan derivatives to exert a synergistic anticancer effect on TNBC cells [32]. Research indicated that blocking ATP synthase using oligomycin could specifically hinder mTORC1 signaling and suppress the proliferation of LAR-subtype TNBC cells [33]. Our research confirmed the therapeutic effect of Oligomycin on TNBC in vitro and in vivo, demonstrating its promising therapeutic potential. All the findings indicated that mitochondrial inhibition could be a potential therapeutic strategy in TNBC.

In conclusion, we identified protein ATP5MF as a key functional protein in non-*BRCA1/BRCA2* TNBC by hdWGCNA and comprehensive analysis. ATP5MF plays a crucial role in the growth and mitochondrial functions of TNBC cells, making it a potential target for therapeutic interventions.

Supplementary Information

The online version contains supplementary material available at https://doi.org/10.1186/s12967-024-05692-9.

Supplementary material 1

Acknowledgements
We thank the associate editor and the reviewers for their useful feedback that improved this paper.

Authors' contributions
Kaiyan Chen: Conceptualization, Methodology and Writing.
Yingchun Wu: Data Curation and Data Analysis.
Linfeng Xu: Investigation, Visualization and Data Presentation.
Changyong Wang: Review and Editing.
Jinqiu Xue: Review, Editing and Funding acquisition.

Funding
This study was supported by the Science and Technology Development Fund of Nanjing Medical University (No.NMUB20230014).

Data availability
Not applicable.

Declarations

Ethics approval and consent to participate
This study was approved by the Ethics Committee of the Second Affiliated Hospital of Nanjing Medical University .

Consent for publication
We declare that the Publisher has the Author's permission to publish the.

Competing interests
The authors declare that they have no competing interests.

Author details
[1]Department of General Surgery, The Second Affiliated Hospital of Nanjing Medical University, Nanjing 210011, Jiangsu, China. [2]The Graduate School of Nanjing Medical University, Nanjing, Jiangsu, China. [3]Ultrasonic Department, The Second Affiliated Hospital of Nanjing Medical University, Nanjing 210011, Jiangsu, China. [4]Nanjing Jinling Hospital, Affiliated Hospital of Medical School, Nanjing University, Nanjing, China.

Received: 25 June 2024 Accepted: 18 September 2024
Published online: 14 October 2024

References

1. Li Y, Zhang H, Merkher Y, Chen L, Liu N, Leonov S, Chen Y. Recent advances in therapeutic strategies for triple-negative breast cancer. J Hematol Oncol. 2022;15:121.
2. Luo L, Keyomarsi K. PARP inhibitors as single agents and in combination therapy: the most promising treatment strategies in clinical trials for BRCA-mutant ovarian and triple-negative breast cancers. Expert Opin Investig Drugs. 2022;31:607–31.
3. Hallett RM, Dvorkin-Gheva A, Bane A, Hassell JA. A gene signature for predicting outcome in patients with basal-like breast cancer. Sci Rep. 2012;2:227.
4. Bonotto M, Gerratana L, Poletto E, Driol P, Giangreco M, Russo S, Minisini AM, Andreetta C, Mansutti M, Pisa FE, Fasola G, Puglisi F. Measures of outcome in metastatic breast cancer: insights from a real-world scenario. Oncologist. 2014;19:608–15.
5. Poggio F, Bruzzone M, Ceppi M, Pondé NF, La Valle G, Del Mastro L, de Azambuja E, Lambertini M. Platinum-based neoadjuvant chemotherapy in triple-negative breast cancer: a systematic review and meta-analysis. Annals Oncology: Official J Eur Soc Med Oncol. 2018;29:1497–508.
6. Denkert C, Liedtke C, Tutt A, von Minckwitz G. Molecular alterations in triple-negative breast cancer-the road to new treatment strategies. Lancet (London England). 2017;389:2430–42.
7. Isakoff SJ, Mayer EL, He L, Traina TA, Carey LA, Krag KJ, Rugo HS, Liu MC, Stearns V, Come SE, Timms KM, Hartman AR, Borger DR, Finkelstein DM, Garber JE, Ryan PD, Winer EP, Goss PE, Ellisen LW. TBCRC009: a multicenter phase II clinical trial of platinum monotherapy with biomarker assessment in metastatic triple-negative breast cancer. J Clin Oncology: Official J Am Soc Clin Oncol. 2015;33:1902–9.
8. Morabito S, Miyoshi E, Michael N, Shahin S, Martini AC, Head E, Silva J, Leavy K, Perez-Rosendahl M, Swarup V. Single-nucleus chromatin accessibility and transcriptomic characterization of Alzheimer's disease. Nat Genet. 2021;53:1143–55.
9. Xu W, Zhang W, Zhao D, Wang Q, Zhang M, Li Q, Zhu W, Xu C. Unveiling the role of regulatory T cells in the tumor microenvironment of pancreatic cancer through single-cell transcriptomics and in vitro experiments. Front Immunol. 2023;14:1242909.
10. Lee AV. Location, location, location: regulation of breast cancer progression by the microenvironment. Breast cancer Research: BCR. 2004;6:279–80.
11. Subramanian A, Narayan R, Corsello SM, Peck DD, Natoli TE, Lu X, Gould J, Davis JF, Tubelli AA, Asiedu JK, Lahr DL, Hirschman JE, Liu Z, Donahue M, Julian B, Khan M, Wadden D, Smith IC, Lam D, Liberzon A, Toder C, Bagul M, Orzechowski M, Enache OM, Piccioni F, Johnson SA, Lyons NJ, Berger AH, Shamji AF, Brooks AN, Vrcic A, Flynn C, Rosains J, Takeda DY, Hu R, Davison D, Lamb J, Ardlie K, Hogstrom L, Greenside P, Gray NS, Clemons

PA, Silver S, Wu X, Zhao WN, Read-Button W, Wu X, Haggarty SJ, Ronco LV, Boehm JS, Schreiber SL, Doench JG, Bittker JA, Root DE, Wong B, Golub TR. A next generation connectivity map: L1000 platform and the first 1,000,000 profiles. Cell. 2017;171:1437-e14521417.
12. Ahmed F, Ho SG, Samantasinghar A, Memon FH, Rahim CSA, Soomro AM, Sunlidutt N, Kim KH, Choi KH. Drug repurposing in psoriasis, performed by reversal of disease-associated gene expression profiles. Comput Struct Biotechnol J. 2022;20:6097–107.
13. Samantasinghar A, Ahmed F, Rahim CSA, Kim KH, Kim S, Choi KH. Artificial intelligence-assisted repurposing of lubiprostone alleviates tubulointerstitial fibrosis. Translational Research: J Lab Clin Med. 2023;262:75–88.
14. Morabito S, Reese F, Rahimzadeh N, Miyoshi E, Swarup V. hdWGCNA identifies co-expression networks in high-dimensional transcriptomics data. Cell Rep Methods. 2023;3:100498.
15. Galber C, Minervini G, Cannino G, Boldrin F, Petronilli V, Tosatto S, Lippe G, Giorgio V. The f subunit of human ATP synthase is essential for normal mitochondrial morphology and permeability transition. Cell Rep. 2021;35:109111.
16. Garrido-Castro AC, Lin NU, Polyak K. Insights into molecular classifications of triple-negative breast cancer: improving patient selection for treatment. Cancer Discov. 2019;9:176–98.
17. Lehmann BD, Bauer JA, Chen X, Sanders ME, Chakravarthy AB, Shyr Y, Pietenpol JA. Identification of human triple-negative breast cancer subtypes and preclinical models for selection of targeted therapies. J Clin Investig. 2011;121:2750–67.
18. Jiang YZ, Ma D, Suo C, Shi J, Xue M, Hu X, Xiao Y, Yu KD, Liu YR, Yu Y, Zheng Y, Li X, Zhang C, Hu P, Zhang J, Hua Q, Zhang J, Hou W, Ren L, Bao D, Li B, Yang J, Yao L, Zuo WJ, Zhao S, Gong Y, Ren YX, Zhao YX, Yang YS, Niu Z, Cao ZG, Stover DG, Verschraegen C, Kaklamani V, Daemen A, Benson JR, Takabe K, Bai F, Li DQ, Wang P, Shi L, Huang W, Shao ZM. Genomic and transcriptomic landscape of triple-negative breast cancers: subtypes and treatment strategies. Cancer cell. 2019;35:428–40.
19. Langfelder P, Horvath S. WGCNA: an R package for weighted correlation network analysis. BMC Bioinformatics. 2008;9:559.
20. Yip AM, Horvath S. Gene network interconnectedness and the generalized topological overlap measure. BMC Bioinformatics. 2007;8:22.
21. Dong J, Horvath S. Understanding network concepts in modules. BMC Syst Biol. 2007;1:24.
22. Langfelder P, Zhang B, Horvath S. Defining clusters from a hierarchical cluster tree: the dynamic Tree Cut package for R. Bioinf (Oxford England). 2008;24:719–20.
23. Butler A, Hoffman P, Smibert P, Papalexi E, Satija R. Integrating single-cell transcriptomic data across different conditions, technologies, and species. Nat Biotechnol. 2018;36:411–20.
24. Stuart T, Butler A, Hoffman P, Hafemeister C, Papalexi E, Mauck WM, Hao Y, Stoeckius M, Smibert P, Satija R. Comprehensive integration of single-cell data. Cell. 2019;177:1888-e19021821.
25. Weinberg SE, Chandel NS. Targeting mitochondria metabolism for cancer therapy. Nat Chem Biol. 2015;11:9–15.
26. Park JH, Vithayathil S, Kumar S, Sung PL, Dobrolecki LE, Putluri V, Bhat VB, Bhowmik SK, Gupta V, Arora K, Wu D, Tsouko E, Zhang Y, Maity S, Donti TR, Graham BH, Frigo DE, Coarfa C, Yotnda P, Putluri N, Sreekumar A, Lewis MT, Creighton CJ, Wong LC. Kaipparettu, fatty acid oxidation-driven src links mitochondrial energy reprogramming and oncogenic properties in triple-negative breast cancer. Cell Reports. 2016;14:2154–65.
27. Luo X, Gong X, Su L, Lin H, Yang Z, Yan X, Gao J. Activatable mitochondria-targeting organoarsenic prodrugs for bioenergetic cancer therapy. Angew Chem Int Ed Engl. 2021;60:1403–10.
28. Zhu YX, Jia HR, Gao G, Pan GY, Jiang YW, Li P, Zhou N, Li C, She C, Ulrich NW, Chen Z, Wu FG. Mitochondria-acting nanomicelles for destruction of cancer cells via excessive mitophagy/autophagy-driven lethal energy depletion and phototherapy. Biomaterials. 2020;232:119668.
29. Jia D, Park JH, Jung KH, Levine H, Kaipparettu BA. Elucidating the metabolic plasticity of cancer: mitochondrial reprogramming and hybrid Metabolic States. Cells. 2018;7(3):21.
30. Zacksenhaus E, Shrestha M, Liu JC, Vorobieva I, Chung PED, Ju Y, Nir U, Jiang Z. Mitochondrial OXPHOS induced by RB1 deficiency in breast cancer: implications for anabolic metabolism, stemness, and metastasis. Trends cancer. 2017;3:768–79.
31. Choi J, Kim DH, Jung WH, Koo JS. Metabolic interaction between cancer cells and stromal cells according to breast cancer molecular subtype. Breast cancer Research: BCR. 2013;15:R78.
32. Zueva AO, Silchenko AS, Rasin AB, Malyarenko OS, Kusaykin MI, Kalinovsky AI, Ermakova SP. Production of high- and low-molecular weight fucoidan fragments with defined sulfation patterns and heightened in vitro anticancer activity against TNBC cells using novel endo-fucanases of the GH107 family. Carbohydr Polym. 2023;318:121128.
33. Kil YS, Risinger AL, Petersen CL, Mooberry SL, Cichewicz RH. Leucinostatins from ophiocordyceps spp. and purpureocillium Spp. demonstrate selective antiproliferative effects in cells representing the luminal androgen receptor subtype of triple negative breast cancer. J Nat Prod. 2020;83:2010–24.

Publisher's note